BMB Reports - Manuscript Submission

Manuscript Draft

Manuscript Number: BMB-22-065

Title: NRF2 activation by 2-methoxycinnamaldehyde attenuates inflammatory responses in macrophages via enhancing autophagy flux

Article Type: Article

Keywords: NRF2; Autophagy; 2-Methoxycinnamaldehyde; Inflammation; LPS

Corresponding Author: Ki-Tae Ha

Authors: Bo-Sung Kim[1,2,#], Minwook Shin[3,#], Kyu-Won Kim[4], Ki-Tae Ha[1,2,*,#], Sung-Jin Bae[5,#]

Institution: [1]Department of Korean Medical Science, School of Korean Medicine and [2]Korean Medical Research Center for Healthy Aging, Pusan National University,
[3]RNA Therapeutics Institute, University of Massachusetts Chan Medical School,
[4]College of Pharmacy and Research Institute of Pharmaceutical Sciences, Seoul National University,
[5]Department of Molecular Biology and Immunology, Kosin University College of Medicine,

Manuscript Type: Article

Title: NRF2 activation by 2-methoxycinnamaldehyde attenuates inflammatory responses in macrophages via enhancing autophagy flux

Authors' name: Bo-Sung Kim[1,2,†], Minwook Shin[3,†], Kyu-Won Kim[4], Ki-Tae Ha[1,2,*], and Sung-Jin Bae[5,*]

[†]These authors contributed equally to this work.

Affiliations:

[1]Department of Korean Medical Science, School of Korean Medicine, Pusan National University, Yangsan, Gyeongnam 50612, Republic of Korea

[2]Korean Medical Research Center for Healthy Aging, Pusan National University, Yangsan, Gyeongnam 50612, Republic of Korea

[3]RNA Therapeutics Institute, University of Massachusetts Chan Medical School, Worcester, MA 01605, USA

[4]College of Pharmacy and Research Institute of Pharmaceutical Sciences, Seoul National University, Seoul 08826, Republic of Korea

[5]Department of Molecular Biology and Immunology, Kosin University College of Medicine, Busan 49267, Republic of Korea

Running Title: NRF2-enhanced autophagy attenuates inflammation

Keywords: NRF2, Autophagy, 2-Methoxycinnamaldehyde, Inflammation, LPS

Corresponding Authors:

Ki-Tae Ha, K.M.D., Ph.D.

Professor

Department of Korean Medical Science

School of Korean Medicine and Korean Medicine Research Center for Healthy Aging

Pusan National University

Yangsan 50612, Republic of Korea

Phone: 82-51-510-8464

Fax: 82-51-510-8420

E-mail: hagis@pusan.ac.kr

Sung-Jin Bae, K.M.D., Ph.D.

Assistant Professor

Department of Molecular Biology and Immunology

Kosin University College of Medicine

Busan 49267, Republic of Korea

Phone: 82-51-990-6418

Fax: 82-51-990-3081

E-mail: Dr.BaeSJ@kosin.ac.kr

ABSTRACT

A well-controlled inflammatory response is crucial for the recovery from injury and maintenance of tissue homeostasis. The anti-inflammatory response of 2-methoxycinnamaldehyde (2-MCA), a natural compound derived from cinnamon, has been studied; however, the underlying mechanism on macrophage has not been fully elucidated. In this study, LPS-stimulated production of TNF-α and NO was reduced by 2-MCA in macrophages. 2-MCA significantly activated the NRF2 pathway, and expression levels of autophagy-associated proteins in macrophages, including LC3 and P62, were enhanced via NRF2 activation regardless of LPS treatment, suggesting the occurrence of 2-MCA-mediated autophagy. Moreover, evaluation of autophagy flux using luciferase-conjugated LC3 revealed that incremental LC3 and P62 levels are coupled to enhanced autophagy flux. Finally, reduced expression levels of TNF-α and NOS2 by 2-MCA were reversed by autophagy inhibitors, such as bafilomycin A1 and NH_4Cl, in LPS-stimulated macrophages. In conclusion, 2-MCA enhances autophagy flux in macrophages via NRF2 activation and consequently reduces LPS-induced inflammation.

INTRODUCTION

Inflammation is an essential response of the body against infection, tissue injury, and cellular stress (1). Among the innate immune cells, macrophages are rapidly recruited and mediate inflammatory responses in infectious diseases (2). Macrophages accomplish the initial microbial defense via tumor necrosis factor-α (TNF-α) and nitric oxide (NO) production (3, 4). A well-controlled inflammatory response, including adequate TNF-α and NO secretion, helps manage pathogenic microbial infection. However, excessive production of these molecules may lead to septic shock. Therefore, the control of inflammation is an important therapeutic target in infectious diseases.

The genus *Cinnamomum* include evergreen trees of about 250 species distributed worldwide. Notably, 2-methoxycinnamaldehyde (2-MCA) is a compound commonly identified in cinnamon (5); its anti-inflammatory, antioxidant, anti-osteoclastogenesis, anti-angiogenesis, and anti-aggregation activities have been studied in various types of cells, including macrophages, endothelial cells, tumor cells, and platelets (6-10). Particularly, it potentiates anti-inflammatory and antioxidant effects in macrophages. However, there is still no clear investigation regarding its mechanism of action.

Nuclear factor erythroid 2-related factor 2 (NRF2) regulates antioxidant gene expression to protect against oxidative damage induced by injury and inflammation (11). For its antioxidant response, NRF2 binds to antioxidant response elements (AREs) in gene promoter regions to produce various enzymes, such as heme oxygenase-1 (HO-1), NADH quinone oxidoreductase 1 (NQO1), and superoxide dismutase (SOD1) (12). Normally, NRF2 in the cytoplasm binds with Kelch-like ECH-associated protein 1 (KEAP1), which performs the ubiquitination and proteolysis of NRF2 (13). On the other hand, autophagosome cargo protein P62/SEQUESTOSOME1 (P62/SQSTM1) acts on KEAP1 at the same binding site as NRF2-KEAP1 to competitively inhibit their interaction, consequently protecting NRF2 from

its degradation (14). Upon stabilization, NRF2 increases the expression level of P62, which interacts with KEAP1 more frequently and further accelerates the activation of free NRF2 (15). Moreover, accumulated P62 and LC3 bind to each other to trigger the autophagosome formation on its membrane (16).

In this study, we demonstrated that the 2-MCA-induced anti-inflammatory effect in macrophages is mediated via NRF2 activation. Furthermore, NRF2-mediated autophagy enhancement could modulate excessive inflammation by diminishing TNF-α and NO production.

RESULTS

2-MCA reduces TNF-α and NO secretion in macrophages

We searched several natural compounds in PubMed by using the following keywords: natural compound, inflammation, phytochemical, and TNF-α. Based on the results, six compounds were selected: β-caryophyllene, hydroxycitric acid, ruscogenin A, maslinic acid, β-myrcene, and 2-MCA (Fig. S1). To confirm the anti-inflammatory effect of each compound in macrophages, we first examined TNF-α production together with the cell viability in lipopolysaccharide (LPS)-stimulated RAW264.7 cells and bone-marrow macrophages (BMMs). In RAW264.7 cells, two compounds, maslinic acid and 2-MCA, significantly reduced TNF-α production (Fig. S2). However, only 2-MCA successfully reduced TNF-α production without significant cell death in LPS-exposed BMMs (Fig. S3). Then, we further examined the concentration-dependent cytotoxicity of 2-MCA in both cells. In all tested conditions, 2-MCA did not affect cell viability (Fig. 1A). Next, concentration-dependent TNF-α and NO secretion levels were measured to ensure the anti-inflammatory effect of 2-MCA. Consistently, 2-MCA inhibited TNF-α and NO secretion in a concentration-dependent manner in LPS-stimulated macrophages, especially from concentrations of 12.5 to

100 μM (Fig. 1B and 1C). As a result, we selected the 50-μM concentration to investigate the anti-inflammatory mechanism of 2-MCA.

2-MCA maintains LPS-induced MAPK, NF-kB, and AP-1 pathways

Next, we evaluated whether 2-MCA primarily affects the well-known LPS-related signaling pathway, including the MAPK, NF-κB, and AP1 pathways. In the MAPK signaling pathway, phosphorylation levels of p38, ERK, and JNK were increased by LPS in both RAW264.7 cells and BMMs; all of them were unchanged by 4-h pretreatment of 2-MCA (Fig. 2A and 2B). Similarly, LPS-initiated degradation of IκB and induction of c-Jun and c-Fos in NF-κB and AP-1 signaling, respectively, were also unaffected by 4-h pretreatment of 2-MCA in macrophages (Fig. 2C and 2D). These data suggest that LPS-induced conventional pathways were not the primary targets in anti-inflammation by 2-MCA.

2-MCA activates NRF2/HO-1 signaling axis in LPS-stimulated macrophages

A previous study revealed that the NRF2/HO-1 pathway was activated in vascular endothelial cells by 2-MCA (17). Thus, we investigated whether 2-MCA would also activate the NRF2/HO-1 pathway in macrophages. We found that 2-MCA activated the NRF2/HO-1 axis, regardless of LPS stimulation (Fig. S4 and S5A). Interestingly, activated NRF2 by 2-MCA further increased ATF3 expression level in LPS-stimulated conditions (Fig. 3A and 3B). In addition, 2-MCA further increased the expression level of HO-1, which was slightly increased by LPS stimulation. On the other hand, LPS-induced NOS2 expression level was significantly decreased by 2-MCA (Fig. 3C and 3D).

Recently, autophagy-associated genes, such as *P62, LC3A/B*, and *ATG5*, have been identified as targets of NRF2 (18, 19). Thus, we further investigated whether such genes could be increased by 2-MCA. We found that the mRNA expression levels of *Sqstm1* and

Map1lc3a, which encode P62 and LC3A, respectively, were sufficiently increased by 2-MCA; results were also similar with ARE activity (Fig. S5). Since P62 and LC3, important proteins for autophagy, are known to be transcribed by both NRF2 and TFEB, we examined whether 2-MCA could activate TFEB-dependent transcription in macrophages. Thus, mRNA expression levels of TFEB-target genes, *Tfeb* and *Lamp2*, were evaluated; no obvious enhancement by 2-MCA was observed (Fig S6A and S6B). Moreover, TFEB activity analysis using 5xCLEAR (Coordinated Lysosomal Expression and Regulation) reporter, which contained five repeats of TFEB-responsive elements (20), showed that rapamycin successfully increased TFEB activity; in contrast, 2-MCA did not demonstrate similar results (Fig. S6C).

Therefore, these data suggest that 2-MCA increases NRF2 activity followed by increasing the expression levels of canonical genes, such as ATF3 and HO-1, and autophagy-associated genes, such as P62 and LC3A.

Elevated autophagy flux by 2-MCA reduces pro-inflammation in LPS-stimulated macrophages

Based on the enhanced expression of autophagy-associated genes, including P62 and LC3A, we evaluated whether their incremental expression could accompany the changes in autophagy flux. Thus, we adopted the luciferase-conjugated LC3 reporter (21). We found that the luciferase-LC3 reporter successfully chased autophagy flux by reporting inverse correlated luminescence signals with changes in autophagy flux; results revealed reduced signals by Earle's balanced salt solution (EBSS) and enhanced signals by bafilomycin A1 (BafA1), which accelerate and diminish during autophagy flux, respectively (Fig. S7). Thus, we evaluated 2-MCA-dependent autophagy flux in LPS-stimulated RAW264.7 cells. Interestingly, LPS diminished autophagy flux, whereas 2-MCA completely enhanced

autophagy flux to levels of the absence of LPS (Fig. 4A).

We investigated whether this increase in autophagy flux was correlated with the anti-inflammatory effect of 2-MCA. We evaluated the mRNA expression levels of *Tnf* and *Nos2* in RAW264.7 cells, which affect TNF-α and NO secretion. As a result, LPS highly elevated *Tnf* and *Nos2* mRNA expression levels, whereas these were significantly diminished by 2-MCA. In addition, BafA1, an autophagy inhibitor that impedes V-ATPase, deteriorated the 2-MCA-induced anti-inflammatory effects to levels of the LPS-only stimulation (Fig. 4B). Moreover, another well-established autophagy inhibitor, NH_4Cl, which prevents lysosomal acidification, also reversed the anti-inflammatory functions of 2-MCA in RAW264.7 cells (Fig. 4C). Therefore, these data suggest that 2-MCA potentiates anti-inflammation via NRF2-mediated enhancement in autophagy flux. Thus, incremental autophagy flux could be strategically used to deal with excessive inflammation.

DISCUSSION

The function of inflammation is to eliminate the initial etiologic cause and repair damaged tissue. This inflammatory response is initiated and amplified by secretory factors, such as TNF-α and NO, released by various immune cells, including macrophages. Therefore, regulating these factors is important to limit the excessive inflammatory response (22, 23). Infection is the entry of pathogenic microorganisms into the body, whether through wounded skin, airways, or other entry points. LPS, an endotoxin which constitutes the outer membrane of bacteria, mediates infectious diseases by triggering an innate immune response within the body (24). In macrophages, LPS activates MAPK, NF-κB, and AP1-related pathways to secrete NO and pro-inflammatory cytokines, such as TNF-α, IL-6, and IL-1 (25-27). Secreted NO promotes the recruitment of circulating immune cells by dilating blood vessels (28). Inflammatory responses by TNF-α and IL-1 mediate recruitment, activation, and adhesion of

circulating phagocytes to remove pathogenic microorganisms (29, 30). However, the uncontrolled hyperinflammatory reaction by cytokine storms and high NO secretions causes high fever, chills, and low blood pressure, which could lead to septic shock (31, 32). Therefore, the appropriate control of inflammation is crucial for treating infectious diseases.

In this regard, we measured the levels of TNF-α and NO, representative factors mediating cytokine storm and low blood pressure, to evaluate the inflammatory response in macrophages. Among the investigated natural compounds expected to regulate hyperinflammation, only 2-MCA significantly reduced TNF-α and NO levels without obvious cytotoxicity. Thus, we deeply investigated how 2-MCA reduces TNF-α and NO levels in macrophages. Our results illustrated that 2-MCA significantly reduced TNF-α and NO levels in macrophages primarily via NRF2 pathway with unaltered conventional LPS-mediated signaling, including MAPK, NF-kB, and AP-1 pathways. Although 2-MCA did not alter the conventional LPS-mediated signaling in a short duration of 4-h pretreatment, the substantial changes due to the secondary effect of NRF2 activation in a longer duration cannot be ruled out. Moreover, autophagy-related genes, such as P62 and LC3A/B, contain AREs in their promoter regions, which induce transcription upon NRF2 stabilization (18, 19). Stabilized NRF2 increases the expression level of P62, which interacts with KEAP1 more frequently and thus further accelerates the activation of free NRF2 (15). Therefore, we confirmed the activation of AREs in response to NRF2 as well as the increased expression levels of P62 and LC3A by 2-MCA. However, 2-MCA did not affect other autophagy-associated genes containing TFEB promoter regions, such as *TFEB* or *LAMP2*.

In the current study, evaluation of autophagy flux using endogenous LC3 proteins was problematic owing to their increased expression levels (Fig. S8). In this case, it is helpful to measure autophagy flux using exogenous LC3, which shows a constant expression level. Previous reports were based on Renilla luciferase-conjugated LC3 (33). On the other hand,

we adopted the firefly luciferase, which is more applicable for luminescence *in vivo* (34). Despite the usage of a different luciferase, our system also reported cellular autophagy flux. Thus, we found that LPS reduces autophagy flux and that 2-MCA successfully ameliorated this process to levels of the absence of LPS. Accordingly, enhanced autophagy suppresses LPS-induced inflammation (35). In addition, autophagy acceleration ameliorated the damage caused by sepsis (36). Together with our current results, autophagy is suspected to reduce inflammation in infectious diseases.

In conclusion, NRF2-associated autophagy flux by 2-MCA successfully reduced macrophage-mediated inflammation. Therefore, NRF2 activation may treat acute infectious diseases by reducing oxidative stress and inducing autophagy flux.

MATERIALS AND METHODS

Cell culture

RAW264.7 cells (Korean Cell Line Bank, Seoul, Korea) were cultured in Dulbecco's Modified Eagle Medium (DMEM; Gibco, Thermo Fisher Scientific, Waltham, MA) at 37 °C containing 5% CO_2, with 10% heat-inactivated fetal bovine serum (FBS; Gibco) and 1% penicillin–streptomycin (Gibco). BMMs were isolated from femurs of mice and cultured in DMEM/F12 medium (GenDEPOT, Barker, TX) at 37 °C containing 5% CO_2, supplemented with 10% FBS, 20% L929-conditioned medium, 1× GlutaMAX (Gibco), and 1% penicillin/streptomycin.

Measurement of TNF-α secretion

To evaluate the effect of 2-MCA, RAW264.7 cells and BMMs were cultured in 96-well plates at 1×10^4 and 2×10^4 cells/well for 12 h. Then, the plates were pre-treated with serially diluted 2-MCA. After a 4-h culture, media was added with or without LPS (1 μg/mL).

After a 24-h incubation period, the cultured supernatant was collected. The amount of secreted TNF-α was measured using Mouse TNF-α ELISA MAX kit (BioLegend, San Diego, CA) according to the manufacturer's instructions.

NO assay

To evaluate the effect of 2-MCA, RAW264.7 cells and BMMs were plated into 60-mm dishes at 5×10^5 and 1×10^6 cells/dish for 12 h and were then pre-treated with serially diluted 2-MCA. After a 4-h culture, media was added with or without LPS (final concentration, 1 μg/mL). After a 24-h incubation period, the cultured supernatant was collected. Cells were then removed via centrifugation at 500 g for 3 min. Then, 100 μL of the cultured supernatant was mixed with 100 μL of Griess reagent (1:1 mixture of 1% sulfanilamide in 30% acetate and 0.1% N-1-naphthyl ethylenediamine dihydrochloride in 60% acetate) at room temperature for 10 min. The absorbance of the incubated samples was measured at 540 nm using a microplate reader. A standard curve drawn with known concentrations of sodium nitrite was applied to calculate the concentration of nitrite, which is the stable end-product.

Luminescence-based autophagy flux analysis

RAW264.7 cells stably expressing luciferase-conjugated LC3 (Fig. S9) were seeded into a white, 96-well plate at 2×10^4 cells/well for 12 h and were then pre-treated with serially diluted 2-MCA. After a 4-h culture, media was added with or without LPS (1 μg/mL) and BafA1 (40 nM). After an 8-h incubation period, the medium was changed to phenol red-free DMEM, which contained *D*-luciferin (100 μg/mL). Upon further incubation at 37 °C for 15 min, luminescence was measured using a microplate reader (Tecan Spark, Tecan, Switzerland).

Statistical analysis

The results are expressed as mean ± standard deviation (SD). Statistical analysis was performed using an unpaired Student's *t*-test or a one-way analysis of variance with Tukey's post-hoc test using GraphPad Prism software (GraphPad Software, La Jolla, CA). The minimum significance level was set at $P = 0.05$; at least three independent replications were performed for each experiment.

ACKNOWLEDGMENTS

M.S., S.-J.B. and K.-W.K. conceived and designed the research. M.S. and B.-S.K. performed the experiments and collected the data. B.-S.K. and S.-J.B. wrote the manuscript. M.S., K.-W.K. and K.-T.H. analyzed the data and revised the manuscript. K.-T.H. and S.-J.B. provided guidance on the study and supervised the project. All the authors reviewed the manuscript and agreed to the submission. This work was supported by a grant from Kosin University College of Medicine (2022) and by the National Research Foundation of Korea (NRF) grants funded by the Korean government (MIST; NRF-2021R1A2B5B01002223 to Kyu-Won Kim, NRF-2020R1C1C1003703 to Sung-Jin Bae, and NRF-2021R1A4A1025662 to Sung-Jin Bae and Ki-Tae Ha).

CONFLICTS OF INTEREST

The authors declare no conflicts of interest.

FIGURE LEGENDS

Fig. 1. Anti-inflammatory effects of 2-MCA in LPS-stimulated macrophages. (A) RAW264.7 cells (left) and BMMs (right) were incubated with 2-MCA as indicated for 24 h. The absorbance produced by MTS was measured at 490 nm. The relative cell viability is shown as the mean ± SD (n = 3, with triplicates in each experiment). (B) RAW264.7 cells (left) and BMMs (right) were pre-incubated with 2-MCA as indicated for 4 h, followed by incubation with or without LPS (1 μg/mL) for 24 h. The secreted TNF-α in the culture media was analyzed by ELISA; $*P < 0.05$, $**P < 0.01$. (C) RAW264.7 (left) and BMMs (right) were incubated with 2-MCA as indicated for 4 h, followed by incubation with or without LPS (1 μg/mL) for 24 h. The released NO was evaluated by Griess Reagent-based analysis; $*P < 0.05$, $**P < 0.01$, $***P < 0.001$.

Fig. 2. Effect of 2-MCA on activation of MAPK, NF-kB, and AP-1 pathways in RAW264.7 and BMMs. (A, B) RAW264.7 cells (A) and BMMs (B) were pre-treated with or without 2-MCA (50 μM) for 4 h. After LPS (1 μg/mL) treatment within the indicated time, the phosphorylation levels p38, p44/42, and JNK were analyzed using immunoblot assay. (C, D) RAW264.7 cells (C) and BMMs (D) were pre-treated with or without 2-MCA (50 μM) for 4 h. After LPS (1 μg/mL) treatment within the indicated time, the phosphorylation levels of IKKα, IKKβ, and p65, degradation of IκBα, and expression levels of c-Jun and c-Fos were analyzed using immunoblot assay.

Fig. 3. Effect of 2-MCA on the expression of NRF2 and ATF3 in RAW264.7. (A) RAW264.7 cells were pre-treated with or without 2-MCA (50 μM) for 4 h. After LPS (1 μg/mL) treatment within the indicated time, the kinetic expression levels of NRF2 and ATF3

were analyzed using immunoblot assay. (B) RAW264.7 cells were pre-treated with or without 2-MCA (50 μM) for 4 h. After LPS (1 μg/mL) treatment within the indicated time, cells were fractionated into cytosol/membrane and nucleus fractions. The nucleus translocations of p65, NRF2, and ATF3 were assessed. (C) RAW264.7 cells, whether pre-treated with or without 2-MCA (50 μM) for 4 h, were stimulated with LPS (1 μg/mL) as indicated. The expression levels of NRF2, ATF3, HO-1, and NOS2 were evaluated using immunoblot assay. (D) RAW264.7 cells, whether pre-incubated with or without 2-MCA as indicated for 4 h, were stimulated with LPS (1 μg/mL) for 4 h. The expression levels of NRF2, ATF3, HO-1, and NOS2 were assessed using immunoblot assay.

Fig. 4. Effects of 2-MCA on Inducing Autophagy Flux in RAW264.7 (A) RAW264.7 cells containing luciferase-LC3 were pre-treated with or without 2-MCA (50 μM) for 4 h. After LPS (1 μg/mL) or BafA1 (40 nM) treatment for 8 h, autophagy flux was measured using luciferase assay. (B, C) RAW264.7 cells were pre-treated with or without 2-MCA (50 μM) for 4 h. After LPS (1 μg/mL), BafA1 (40 nM), or NH_4Cl (10 mM) treatment for 8 h, the expression levels of *Tnf* and *Nos2* were analyzed using qRT-PCR assay. The results from three independent experiments are presented as means ± SD. $*P < 0.05$, $**P < 0.01$ and $***P < 0.001$.

REFERENCES

1. Medzhitov R (2008) Origin and physiological roles of inflammation. Nature 454, 428-435
2. Ley K, Laudanna C, Cybulsky MI and Nourshargh S (2007) Getting to the site of inflammation: the leukocyte adhesion cascade updated. Nat Rev Immunol 7, 678-689
3. Guzik TJ, Korbut R and Adamek-Guzik T (2003) Nitric oxide and superoxide in inflammation and immune regulation. J Physiol Pharmacol 54, 469-487
4. Kalliolias GD and Ivashkiv LB (2016) TNF biology, pathogenic mechanisms and emerging therapeutic strategies. Nat Rev Rheumatol 12, 49-62
5. Rao PV and Gan SH (2014) Cinnamon: a multifaceted medicinal plant. Evid Based Complement Alternat Med 2014, 642942
6. Kim NY, Trinh NT, Ahn SG and Kim SA (2020) Cinnamaldehyde protects against oxidative stress and inhibits the TNFalphainduced inflammatory response in human umbilical vein endothelial cells. Int J Mol Med 46, 449-457
7. Tsuji-Naito K (2008) Aldehydic components of cinnamon bark extract suppresses RANKL-induced osteoclastogenesis through NFATc1 downregulation. Bioorg Med Chem 16, 9176-9183
8. Yamakawa D, Kidoya H, Sakimoto S, Jia W and Takakura N (2011) 2-Methoxycinnamaldehyde inhibits tumor angiogenesis by suppressing Tie2 activation. Biochem Biophys Res Commun 415, 174-180
9. Tsai KD, Cherng J, Liu YH et al (2016) Cinnamomum verum component 2-methoxycinnamaldehyde: a novel antiproliferative drug inducing cell death through targeting both topoisomerase I and II in human colorectal adenocarcinoma COLO 205 cells. Food Nutr Res 60, 31607
10. Kim SY, Koo YK, Koo JY et al (2010) Platelet anti-aggregation activities of compounds from Cinnamomum cassia. J Med Food 13, 1069-1074
11. Kim GY, Jeong H, Yoon HY et al (2020) Anti-inflammatory mechanisms of suppressors of cytokine signaling target ROS via NRF-2/thioredoxin induction and inflammasome activation in macrophages. BMB Rep 53, 640-645
12. Ma Q (2013) Role of Nrf2 in Oxidative Stress and Toxicity. Annual Review of Pharmacology and Toxicology 53, 401-426
13. Bellezza I, Giambanco I, Minelli A and Donato R (2018) Nrf2-Keap1 signaling in oxidative and reductive stress. Biochim Biophys Acta Mol Cell Res 1865, 721-733
14. Baird L and Yamamoto M (2020) The Molecular Mechanisms Regulating the KEAP1-NRF2 Pathway. Mol Cell Biol 40, e00099-00020
15. Jain A, Lamark T, Sjottem E et al (2010) p62/SQSTM1 is a target gene for transcription factor NRF2 and creates a positive feedback loop by inducing antioxidant response element-driven gene transcription. J Biol Chem 285, 22576-22591
16. Pankiv S, Clausen TH, Lamark T et al (2007) p62/SQSTM1 binds directly to Atg8/LC3 to facilitate degradation of ubiquitinated protein aggregates by autophagy. J Biol Chem 282, 24131-24145
17. Hwa JS, Jin YC, Lee YS et al (2012) 2-methoxycinnamaldehyde from Cinnamomum cassia reduces rat myocardial ischemia and reperfusion injury in vivo due to HO-1 induction. J Ethnopharmacol 139, 605-615
18. Jiang T, Harder B, Rojo de la Vega M, Wong PK, Chapman E and Zhang DD (2015)

p62 links autophagy and Nrf2 signaling. Free Radic Biol Med 88, 199-204
19. Frias DP, Gomes RLN, Yoshizaki K et al (2020) Nrf2 positively regulates autophagy antioxidant response in human bronchial epithelial cells exposed to diesel exhaust particles. Sci Rep 10, 3704
20. Palmieri M, Impey S, Kang H et al (2011) Characterization of the CLEAR network reveals an integrated control of cellular clearance pathways. Hum Mol Genet 20, 3852-3866
21. Park GT, Yoon JW, Yoo SB et al (2021) Echinochrome A Treatment Alleviates Fibrosis and Inflammation in Bleomycin-Induced Scleroderma. Mar Drugs 19
22. Mao K, Chen S, Chen M et al (2013) Nitric oxide suppresses NLRP3 inflammasome activation and protects against LPS-induced septic shock. Cell Res 23, 201-212
23. Choi H and Shin EC (2022) Hyper-inflammatory responses in COVID-19 and anti-inflammatory therapeutic approaches. BMB Rep 55, 11-19
24. Matsuura M (2013) Structural Modifications of Bacterial Lipopolysaccharide that Facilitate Gram-Negative Bacteria Evasion of Host Innate Immunity. Front Immunol 4, 109
25. Kwon DJ, Bae YS, Ju SM, Youn GS, Choi SY and Park J (2014) Salicortin suppresses lipopolysaccharide-stimulated inflammatory responses via blockade of NF-kappaB and JNK activation in RAW 264.7 macrophages. BMB Rep 47, 318-323
26. Harada K, Ohira S, Isse K et al (2003) Lipopolysaccharide activates nuclear factor-kappaB through toll-like receptors and related molecules in cultured biliary epithelial cells. Lab Invest 83, 1657-1667
27. Hattori Y, Hattori S and Kasai K (2003) Lipopolysaccharide activates Akt in vascular smooth muscle cells resulting in induction of inducible nitric oxide synthase through nuclear factor-kappa B activation. Eur J Pharmacol 481, 153-158
28. Wink DA, Hines HB, Cheng RY et al (2011) Nitric oxide and redox mechanisms in the immune response. J Leukoc Biol 89, 873-891
29. Parameswaran N and Patial S (2010) Tumor necrosis factor-alpha signaling in macrophages. Crit Rev Eukaryot Gene Expr 20, 87-103
30. Gabay C, Lamacchia C and Palmer G (2010) IL-1 pathways in inflammation and human diseases. Nat Rev Rheumatol 6, 232-241
31. Chousterman BG, Swirski FK and Weber GF (2017) Cytokine storm and sepsis disease pathogenesis. Semin Immunopathol 39, 517-528
32. Titheradge MA (1999) Nitric oxide in septic shock. Biochim Biophys Acta 1411, 437-455
33. Farkas T and Jaattela M (2017) Renilla Luciferase-LC3 Based Reporter Assay for Measuring Autophagic Flux. Methods Enzymol 588, 1-13
34. Kim JE, Kalimuthu S and Ahn BC (2015) In vivo cell tracking with bioluminescence imaging. Nucl Med Mol Imaging 49, 3-10
35. Zeng M, Sang W, Chen S et al (2017) 4-PBA inhibits LPS-induced inflammation through regulating ER stress and autophagy in acute lung injury models. Toxicol Lett 271, 26-37
36. Feng Y, Liu B, Zheng X, Chen L, Chen W and Fang Z (2019) The protective role of autophagy in sepsis. Microb Pathog 131, 106-111

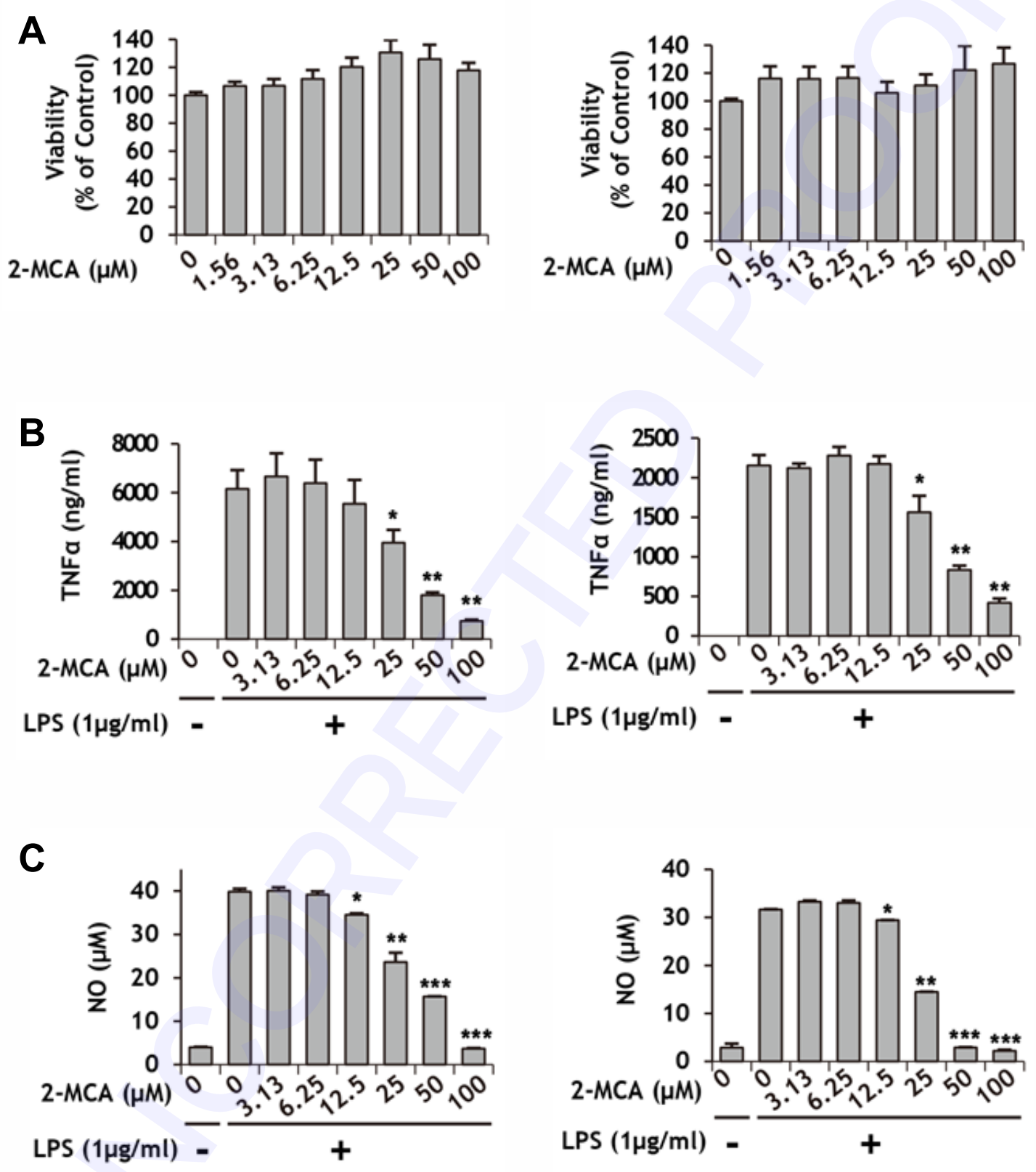

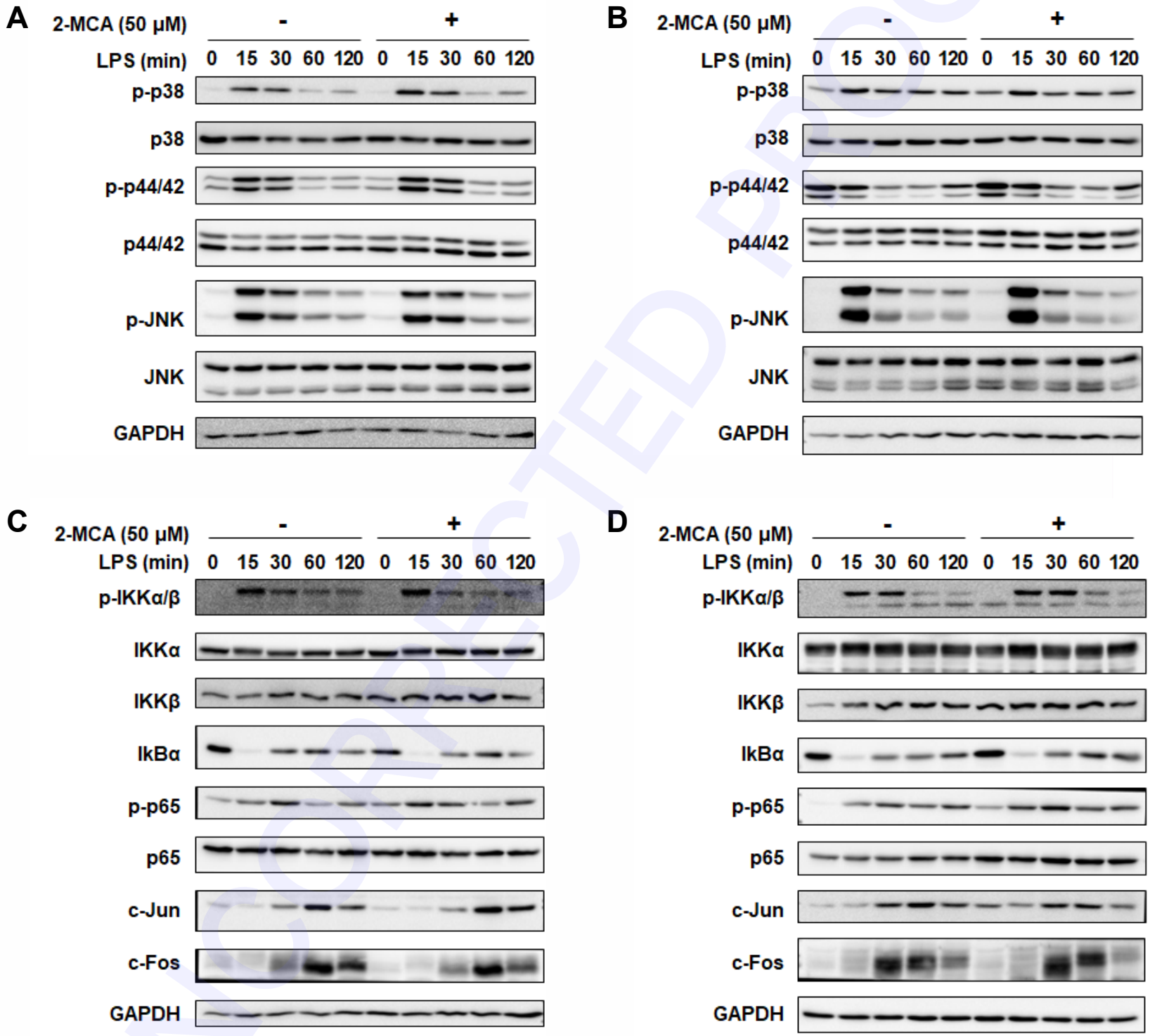

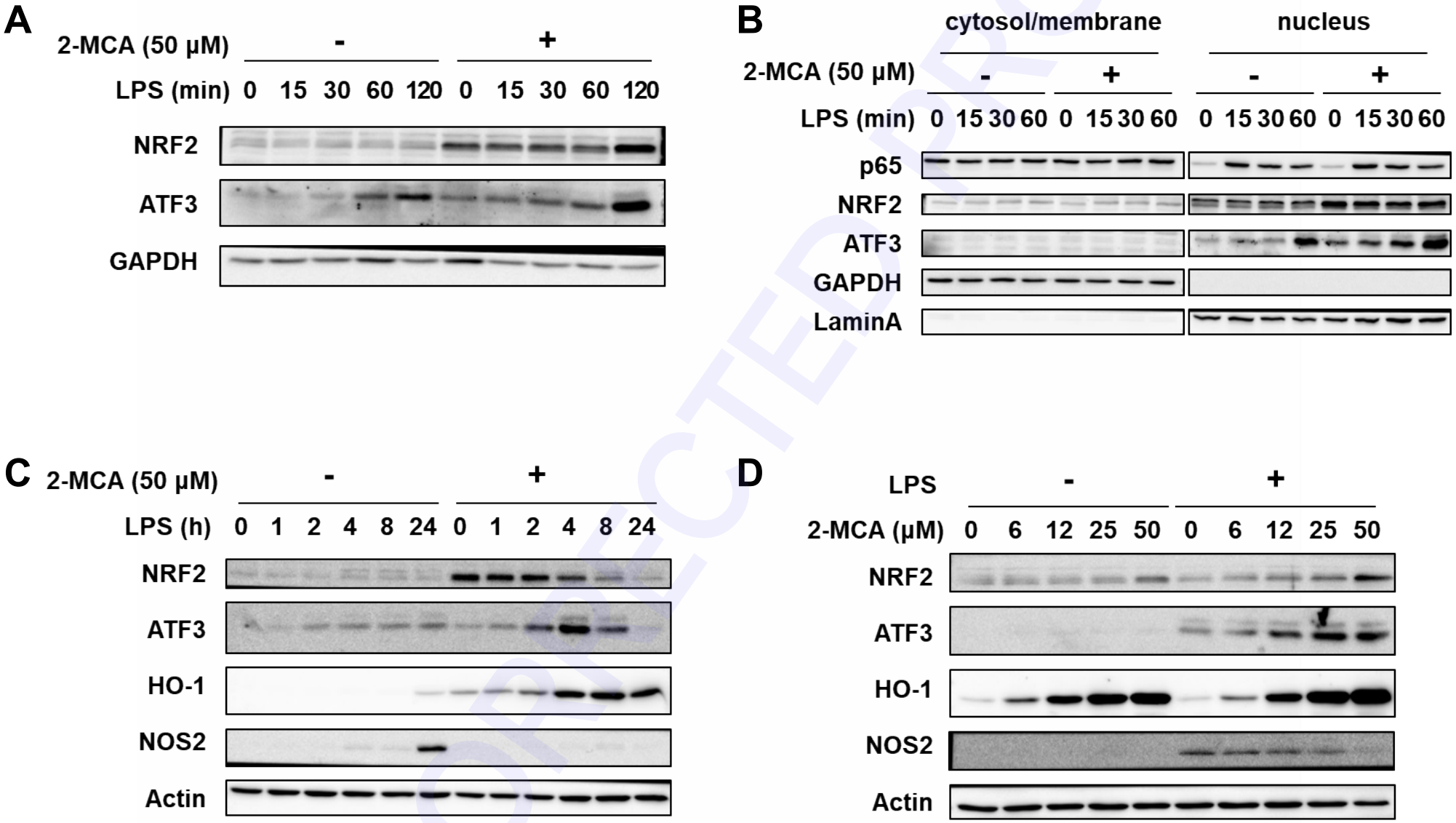

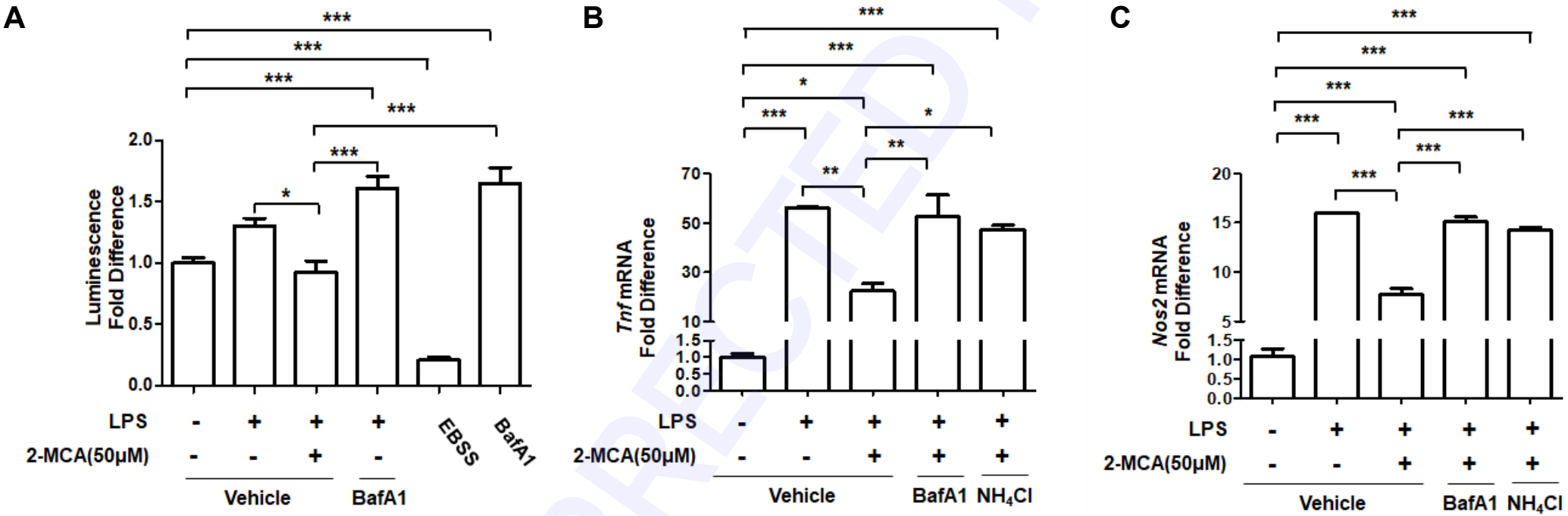

SUPPLEMENTARY MATERIAL

NRF2 activation by 2-methoxycinnamaldehyde attenuates inflammatory responses in macrophages via enhancing autophagy flux

Bo-Sung Kim[1,2,†], Minwook Shin[3,†], Kyu-Won Kim[4], Ki-Tae Ha[1,2,*], and Sung-Jin Bae[5,*]

[†]These authors contributed equally to this work.

Affiliation:

[1]Department of Korean Medical Science, School of Korean Medicine, Pusan National University, Yangsan, Gyeongnam 50612, Republic of Korea

[2]Korean Medical Research Center for Healthy Aging, Pusan National University, Yangsan, Gyeongnam 50612, Republic of Korea

[3]RNA Therapeutics Institute, University of Massachusetts Chan Medical School, Worcester, MA 01605, USA

[4]College of Pharmacy and Research Institute of Pharmaceutical Sciences, Seoul National University, Seoul 08826, Republic of Korea

[5]Department of Molecular Biology and Immunology, Kosin University College of Medicine, Busan 49267, Republic of Korea

SUPPLEMENTARY METHODS

Reagents and antibodies

3-(4,5-dimethylthiazol-2-yl)-5-(3-carboxymethoxyphenyl)-2-(4-sulfophenyl)-2H-tetrazolium (MTS) was supplied by Promega (Madison, WI). All reagents, including D-luciferin, 2-MCA, and LPS, were purchased from Sigma-Aldrich (St. Louis, MO) unless indicated otherwise. The antibodies used in the study are shown in Table S1.

Mice

Male C57BL/6 mice (6-week-old, 20–24 g) were purchased from Orient Bio Inc. (Seongnam, Korea). Mice were provided a standard diet with drinking water before the experiment. All mice were housed in laboratory cage rack systems maintained at a constant temperature (22 ± 1 °C). The rooms were maintained under a 12 h dark/light cycle. All experimental procedures followed the Guidelines for the Care and Use of Laboratory Animals of the National Institutes of Health of Korea and were approved by the Institutional Animal Care and Use Committee of Pusan National University (protocol PNU-2019-2235, approved on March 24, 2019).

Cell viability assay

RAW264.7 cells and BMMs were seeded into 96-well plates at 1×10^4 and 2×10^4 cells/well, respectively. After a 12 h incubation period, serially diluted 2-MCA was treated for 24 h. Cell viability was measured by MTS reduction. The culture medium was changed to an

MTS-containing medium and incubated for 1 h prior to MTS reduction by viable cell dehydrogenases. The soluble formazan product of MTS was measured at 490 nm.

Immunoblot analysis

Proteins were extracted using cell lysis buffer containing 50 mM Tris-Cl (pH 7.4), 300 mM NaCl, 5 mM EDTA, 0.02% (w/v) sodium azide, 1% (w/v) Triton X-100, 10 mM iodoacetamide, 1 mM phenylmethanesulfonyl fluoride, 2 μg/mL leupeptin, and an inhibitor cocktail of protease and phosphatase (Calbiochem, Billerica, MA). Lysates were separated with SDS-PAGE and transferred to a nitrocellulose membrane (GE Healthcare Life Sciences, Pittsburgh, PA). The transferred membrane was probed with specific antibodies. The images were acquired using an LAS4000 machine (GE Healthcare Life Sciences). The antibodies used in the study are shown in Table S1.

RNA isolation and qRT-PCR

Total RNA was isolated from RAW264.7 cells using a GeneJET RNA Purification Kit (ThermoFisher Scientific). Equal amounts of total RNA (1 μg) from each sample were then subjected to reverse transcription using oligo-dT primers with M-MLV reverse transcriptase (ThermoFisher Scientific). Quantitative real-time PCR was performed through the StepOnePlus Real-Time PCR system (Applied Biosystems, Foster City, CA) using the RealHelix qPCR kit (NanoHelix, Seoul, Korea). Relative mRNA levels were normalized using 18S rRNA. The primers used in the study are shown in Table S2.

Promoter activity analysis

RAW264.7 cells containing a fluorescent promoter activity reporter (Fig. S9) were seeded into a 6–well plate at 5×10^5 cells/well for 12 h and treated with 2-MCA (50 μM) or rapamycin (1 μM), as indicated. Promoter activity was measured by qRT-PCR using the mCherry/mCerulean ratio. The TRE sequences are presented in Table S3.

SUPPLEMENTARY FIGURES

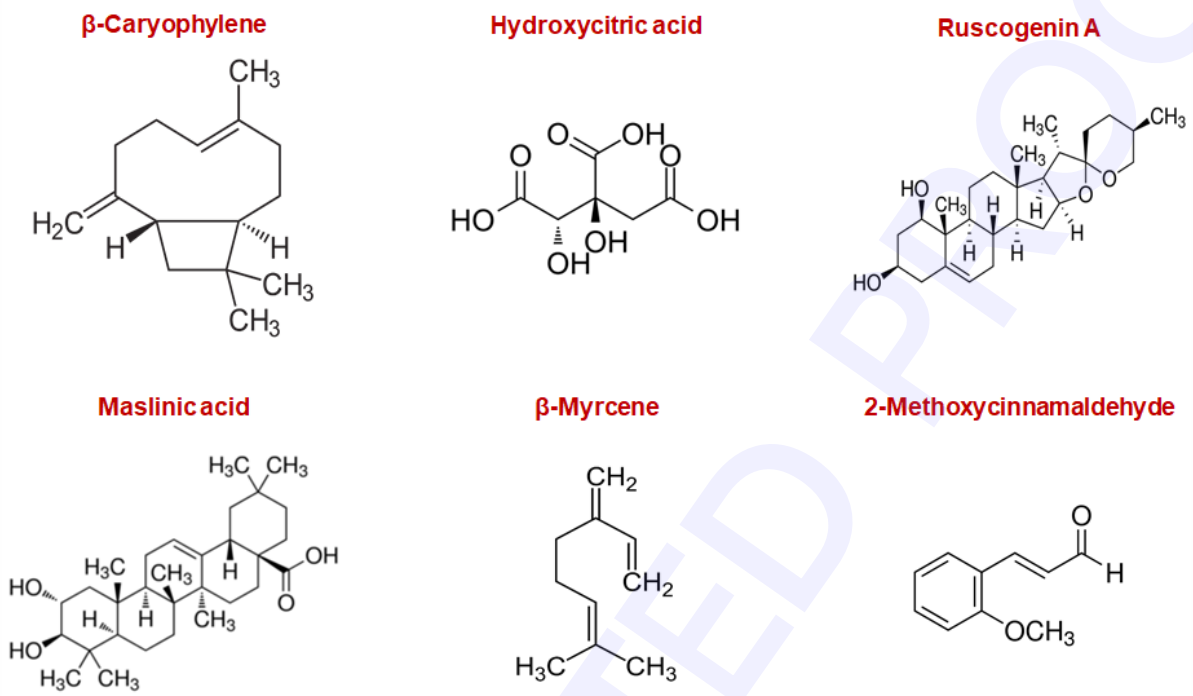

Figure S1. The structure of compounds derived from natural products used in this study.

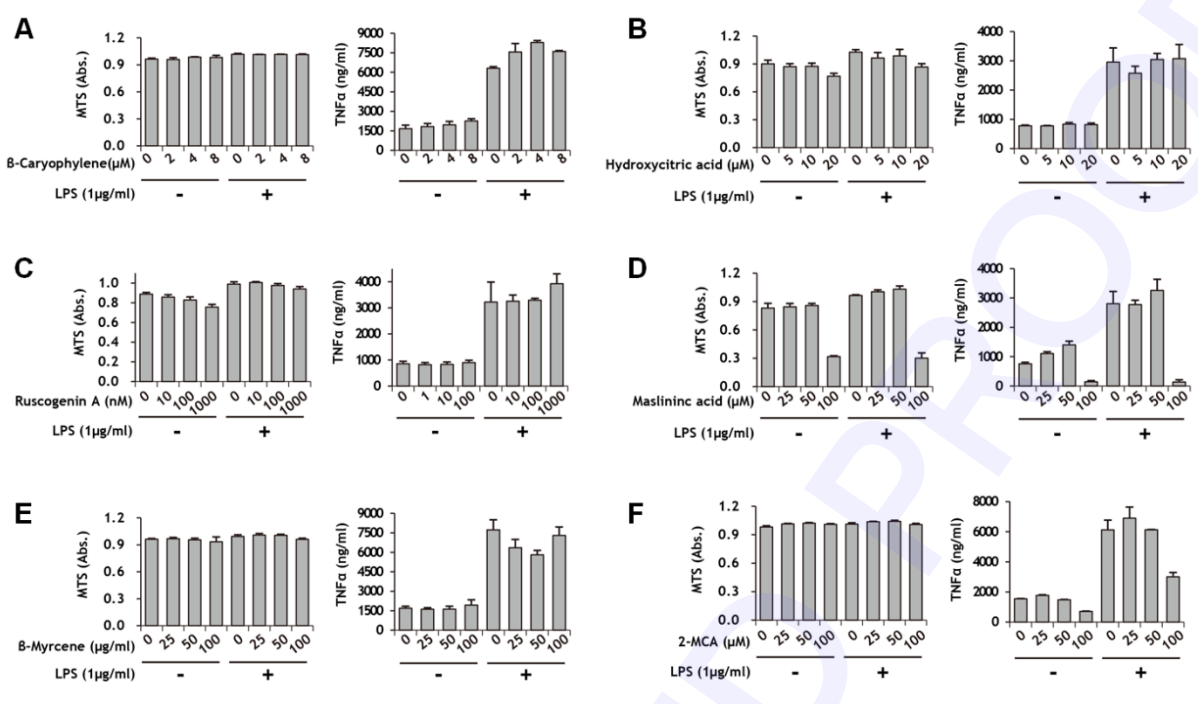

Figure S2. Screening of natural compounds in RAW264.7. RAW264.7 cells were incubated with (A) β-caryophyllene, (B) hydroxycitric acid, (C) ruscogenin A, (D) maslinic acid, (E) β-myrcene, and (F) 2-MCA as indicated for 24 h. The absorbance produced by MTS was measured at 492 nm (left). To analyze TNF-α secretion, RAW264.7 cells were pre-incubated with β-caryophyllene, hydroxycitric acid, ruscogenin A, maslinic acid, β-myrcene, and 2-MCA as indicated for 4 h, followed by incubation with or without LPS (1 μg/mL) for 24 h. The secreted TNF-α level in culture media was analyzed using ELISA (right).

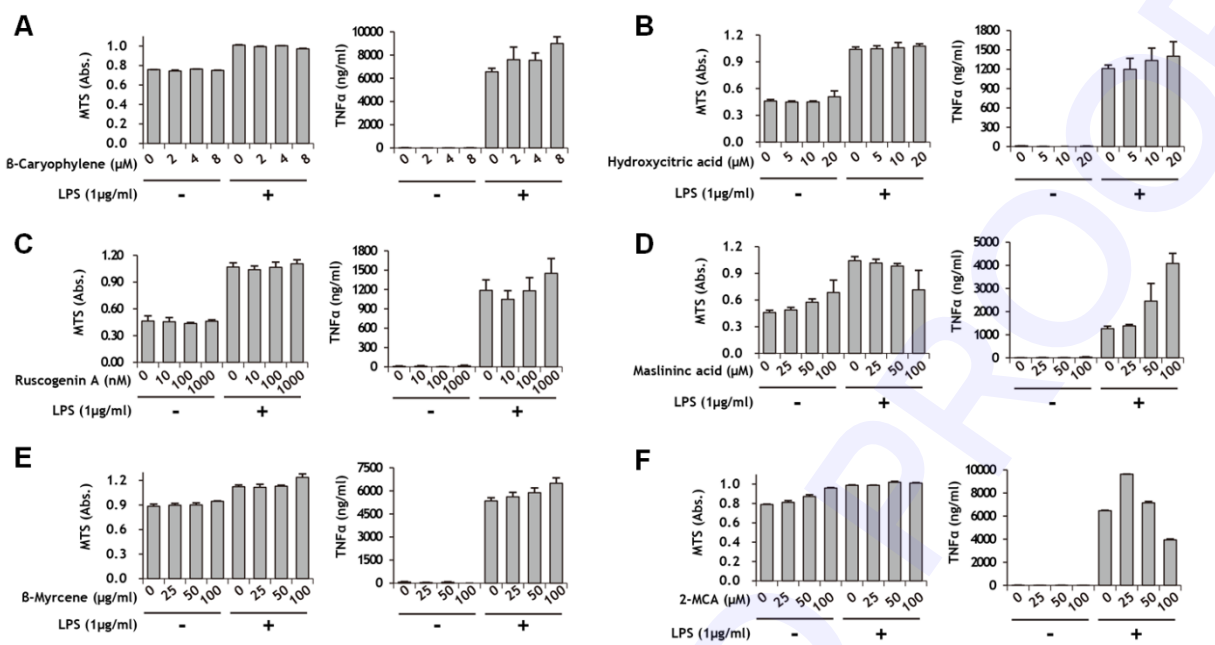

Figure S3. Screening natural compounds in BMMs. BMMs were incubated with (A) β-caryophyllene, (B) hydroxycitric acid, (C) ruscogenin A, (D) maslinic acid, (E) β-myrcene, and (F) 2-MCA as indicated for 24 h. The absorbance induced by MTS was measured at 492 nm (left). To analyze TNF-α secretion, BMMs were pre-incubated with β-caryophyllene, hydroxycitric acid, ruscogenin A, maslinic acid, β-myrcene, and 2-MCA as indicated for 4 h, followed by incubation with or without LPS (1 μg/mL) for 24 h. The secreted TNF-α level in culture media was analyzed using ELISA (right).

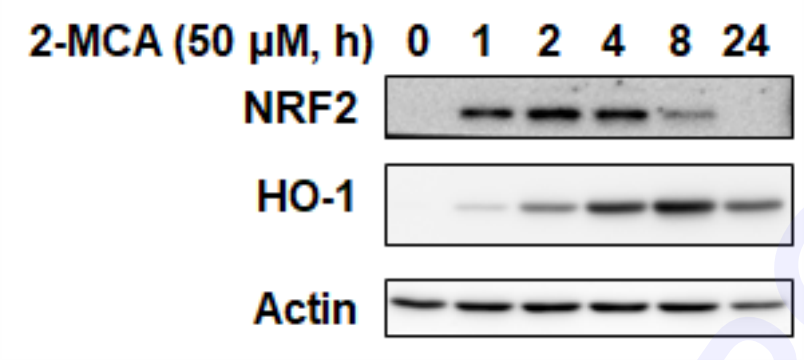

Figure S4. 2-MCA induced the activation of the Nrf2/HO-1 axis in RAW264.7. RAW264.7 cells were treated with 2-MCA (50 μM) for the indicated time. The kinetic expression levels of Nrf2 and HO-1 were analyzed using immunoblot assays.

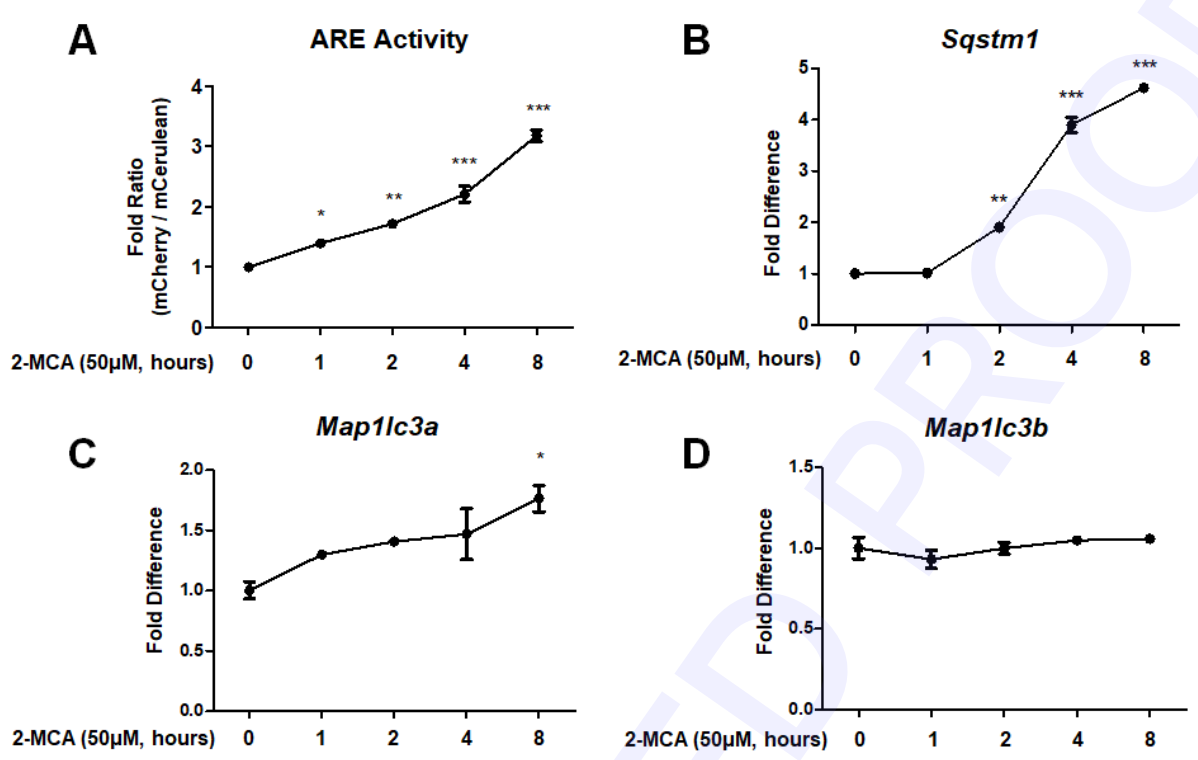

Figure S5. NRF2-dependent gene expression by 2-MCA. (A) RAW264.7 cells containing fluorescent ARE activity reporter were treated with 2-MCA (50 μM) for the indicated time. Activation of the ARE promoter regions was analyzed using qRT-PCR assay. (B–D) RAW264.7 cells were treated with 2-MCA (50 μM) for the indicated time. The expression levels of Sqstm 1, Map1lc3a and Map1lc3b were analyzed using qRT-PCR assay. The results from three independent experiments are presented as mean ± SD. **P* < 0.05, ***P* < 0.01 and ****P* < 0.001.

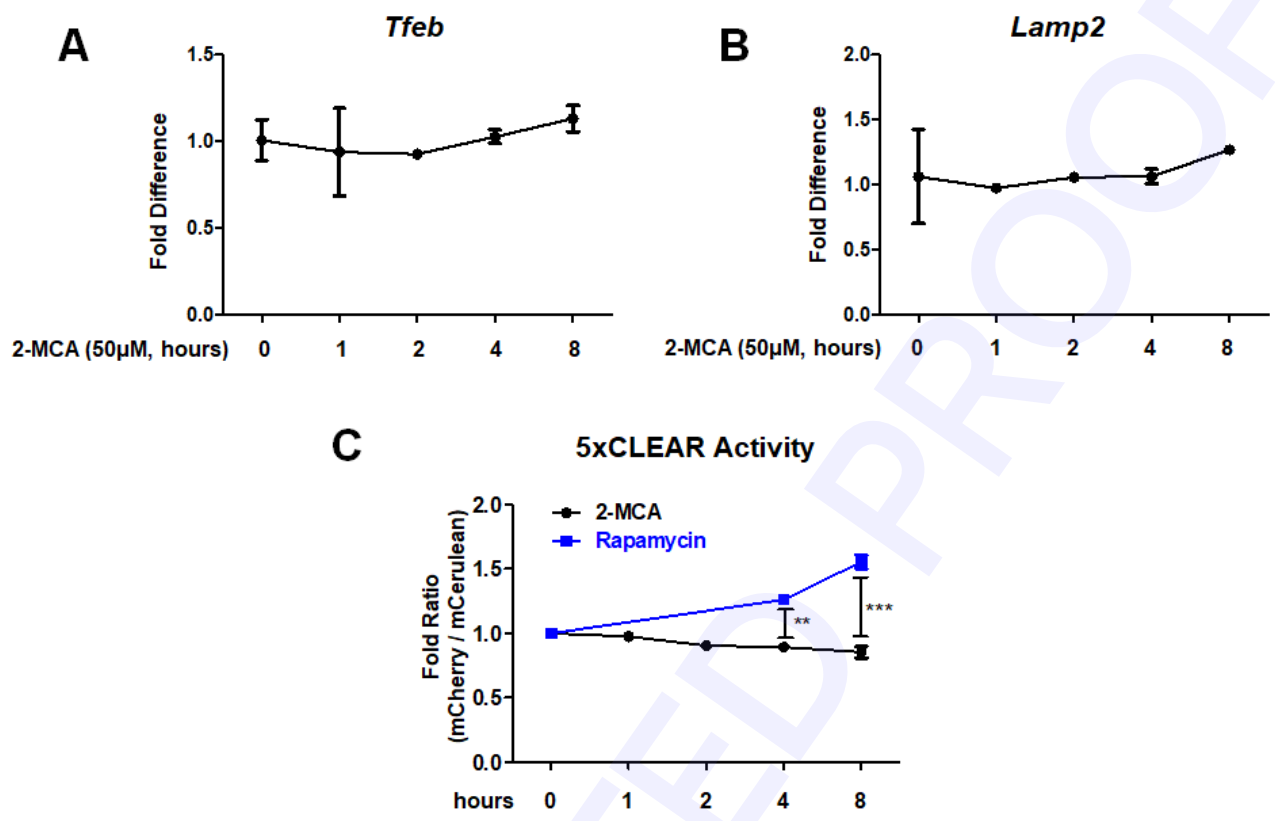

Figure S6. TFEB-dependent gene expression by 2-MCA. (A, B) RAW264.7 cells were treated with 2-MCA (50 μM) for the indicated time. The expression levels of Tfeb, and Lamp2 were analyzed using qRT-PCR assay. (C) RAW264.7 cells containing fluorescent 5xCLEAR activity reporter were treated with 2-MCA (50 μM) and rapamycin (1 μM) for the indicated time. Activation of the 5xCLEAR was analyzed using qRT-PCR assay. The results from three independent experiments are presented as mean ± SD. **P*<0.05, ***P*<0.01 and ****P*<0.001.

.

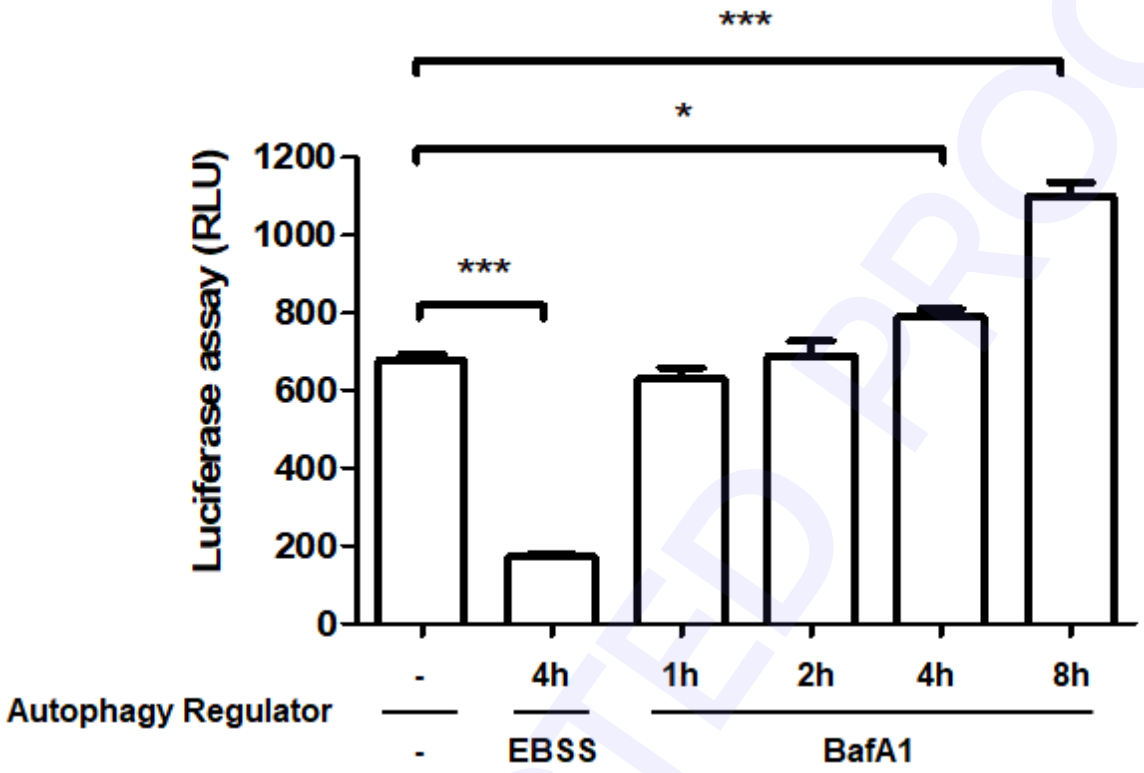

Figure S7. RAW264.7 cells expressing luciferase conjugates LC3 were treated with EBSS and BafA1 (40 nM) for the indicated time. Autophagy flux was measured using luminescence. The results from three independent experiments are presented as means ± SD. **P* < 0.05, ***P* < 0.01 and ****P* < 0.001.

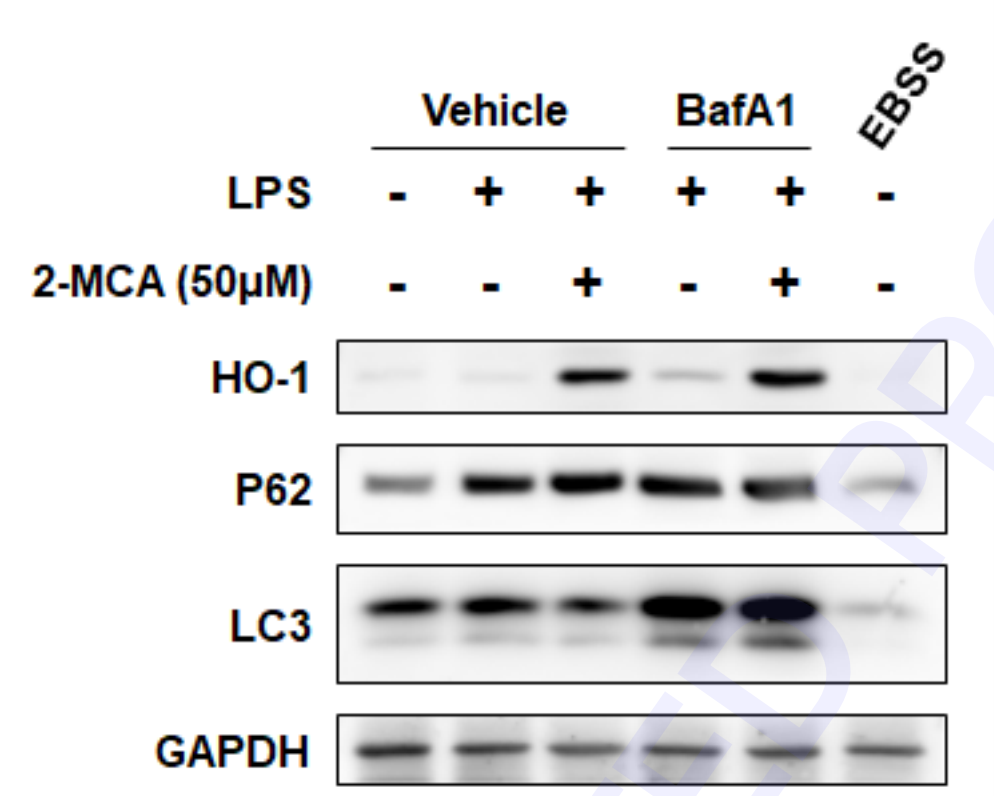

Figure S8. 2-MCA induced autophagy flux in RAW264.7. RAW264.7 cells were pre-treated with or without 2-MCA (50 μM) for 4 h. After LPS (1 μg/mL), BafA1 (40 nM), and EBSS treatment as indicated for 8 h, the kinetic expression levels of HO-1, P62, and LC3 were analyzed using immunoblot assay.

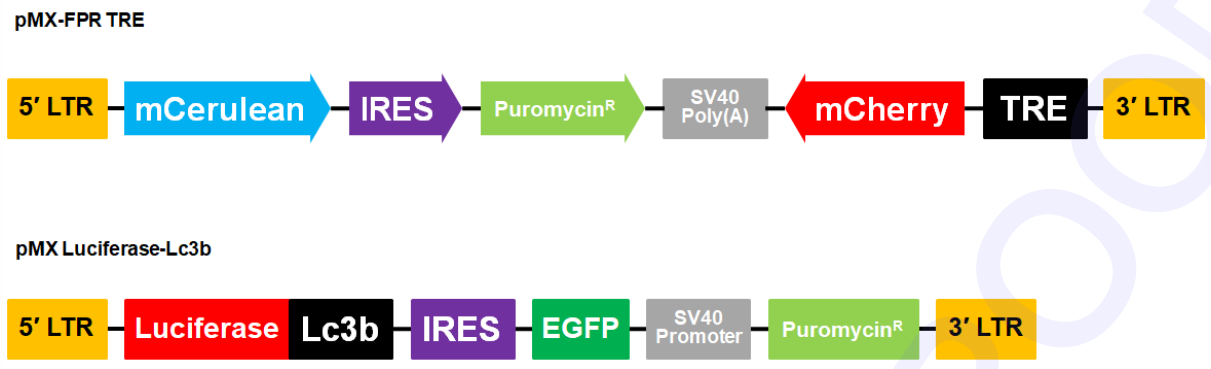

Figure S9. Schematic illustration of retroviral vectors.

SUPPLEMENTARY TABLES

Table S1. Antibodies used.

Antigen	Company	Catalog Number	Dilution Ratio
NOS2	BD Bioscience	610328	1:1000
MYC	Santa Cruz	sc-42	1:1000
GAPDH	Santa Cruz	sc-365062	1:1000
c-JUN	Santa Cruz	sc-74543	1:1000
c-FOS	Santa Cruz	sc-271243	1:1000
ATF3	Santa Cruz	sc-518032	1:1000
Lamin A	Santa Cruz	sc-71481	1:1000
β-actin	Santa Cruz	sc-8432	1:1000
p38	Cell Signaling	#9212	1:1000
p-p38 (Thr180/Tyr182)	Cell Signaling	#9211	1:1000
p44/42	Cell Signaling	#9102	1:1000
p-p44/42 (Thr202/Tyr204)	Cell Signaling	#9101	1:1000
JNK	Cell Signaling	#9252	1:1000
p-JNK (Thr183/Tyr185)	Cell Signaling	#9251	1:1000
IKKα	Cell Signaling	#2682	1:1000
IKKβ	Cell Signaling	#8943	1:1000
p-IKKα/β (Ser176/Ser180)	Cell Signaling	#2697	1:1000
IκBα	Cell Signaling	#9242	1:1000
p65	Cell Signaling	#6956	1:1000
p-p65 (Ser536)	Cell Signaling	#3031	1:1000
Nrf2	Cell Signaling	#20733	1:1000
LC3 A/B	Cell Signaling	#12741	1:1000
HO-1	Enzo Life Sciences	ADI-SPA-895	1:1000
Anti-mouse IgG	Invitrogen	#RJ240410	1:4000
Anti-rabbit IgG	Invitrogen	#SA245916	1:4000

Table S2. Sequence of primers for qRT-PCR.

Gene	Forward (5′ → 3′)	Reverse (5′ → 3′)
Tnf	ATCCGCGACGTGGAACTG	ACCGCCTGGAGTTCTGGAA
Nos2	GGCAGCCTGTGAGACCTTTG	TGCATTGGAAGTGAAGCGTTT
Sqstm1	AGGATGGGGACTTGGTTGC	TCACAGATCACATTGGGGTGC
Map1lc3a	GACCGCTGTAAGGAGGTGC	CTTGACCAACTCGCTCATGTTA
Map1lc3b	GATAATCAGACGGCGCTTGC	ACTTCGGAGATGGGAGTGGA
Tfeb	GGCGCCTGGAGATGACTAAC	ACTGGGCAACTCTTGCTTCA
Lamp2	AGGAGCCGTTCAGTCCAATG	GTGTGTCGCCTTGTCAGGTA
mCerulean	CCCGACAACCACTACCTGAG	TTGTACAGCTCGTCCATGCC
mCherry	ACCTACAAGGCCAAGAAGCC	GGTGTAGTCCTCGTTGTGGG
18S rRNA	GTAACCCGTTGAACCCCATT	CCATCCAATCGGTAGTAGCG

Table S3. TRE Sequence cloned in pMX-FPR.

TRE Name	Element Sequence	Repeats
5xCLEAR	GTCACGTGAC	5
ARE	TCACAGTGACTCAGCAAAATT	3